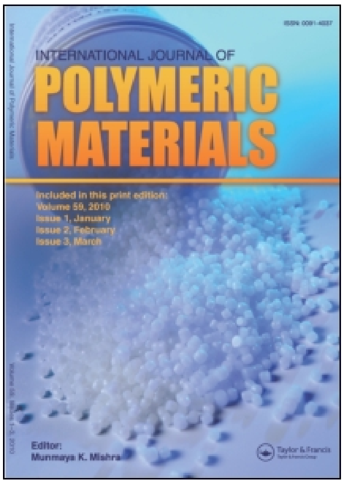

International Journal of Polymeric Materials
Publication details, including instructions for authors and subscription information:
http://www.informaworld.com/smpp/title~content=t713647664

Isothermal Curing Kinetics and Thermal Degradation of o-CFER/MeTHPA/O-MMT Nanocomposite

Jun-gang Gao[a]; Min Zhao[b]
[a] College of Chemistry and Environmental Science, Hebei University, Hebei, People's Republic of China [b] Institute of 42 Industry, Xiangfan, People's Republic of China

To cite this Article Gao, Jun-gang and Zhao, Min(2008) 'Isothermal Curing Kinetics and Thermal Degradation of o-CFER/MeTHPA/O-MMT Nanocomposite', International Journal of Polymeric Materials, 57: 2, 101 — 113
To link to this Article: DOI: 10.1080/00914030701389621
URL: http://dx.doi.org/10.1080/00914030701389621

International Journal of Polymeric Materials, 57:101–113, 2008

ISSN: 0091-4037 print/1563-535X online
DOI: 10.1080/00914030701389621

Isothermal Curing Kinetics and Thermal Degradation of o-CFER/MeTHPA/O-MMT Nanocomposite

Jun-gang Gao
College of Chemistry and Environmental Science, Hebei University, Hebei, People's Republic of China

Min Zhao
Institute of 42 Industry, Xiangfan, People's Republic of China

The isothermal curing kinetics of nanocomposite of o-cresol-formaldehyde epoxy resin (o-CFER), 3-methyl-tetrahydrophthalic anhydride (MeTHPA) with organic montmorillonite (O-MMT) were investigated by means of X-ray diffraction (XRD) and differential scanning calorimetry (DSC) using N,N-dimethyl-benzylamine as a curing accelerant. The XRD result indicates that an exfoliated O-MMT nanocomposite was obtained. The analysis of DSC data indicated that an autocatalytic behavior appeared in the first stages of the cure for the system, which could be well described by the Kamal model. In the later stages, the reaction is mainly controlled by diffusion and a diffusion factor, $f(\alpha)$, was introduced into Kamal's equation. In this way, the curing kinetics were predicted well over the entire range of conversion. The thermal degradation kinetics of this composite were investigated by thermogravimetric analysis (TGA), which revealed that with increasing O-MMT content, TG curves shift to higher temperature.

Keywords: 3-methyl-tetrahydrophthalic anhydride, montmorillonite, o-cresol epoxy resin, reaction kinetics, thermal degradation

INTRODUCTION

Composite materials, in which inorganic filler is dispersed within the polymer matrix on a nanometer scale, are called nanocomposites. The epoxy resins nanocomposites have recently been widely studied, principally due to the far-ranging application potential in many fields.

Received 10 March 2007; in final form 26 March 2007.

Address correspondence to Jun-Gang Gao, College of Chemistry and Environmental Science, Hebei University, Hebei, Baoding 071002, People's Republic of China. E-mail: gaojg@mail.hbu.edu.cn

The nature and mechanism of the exfoliation process of the surface-modified layered-silicate nanoparticles in the crosslinking epoxy network have been of recent interest. Lan [1] demonstrated that the exfoliation of the clay is not only dependent on the reactivity of the epoxy system but also on the rate of intercalation of epoxy and curing agent. Kornmann [2] had compared the effect of aliphatic diamine and cycloaliphatic diamines on the structure of a nanocomposite, and found that while the former gave the slowest cure rate, it allowed more curing agent to penetrate the epoxy swollen galleries and initiate intragallery polymerization leading to better exfoliation, which may be attributed to its characteristic of a more flexible backbone than the cycloaliphatic ones. Monolithic epoxy exfoliated-clay nanocomposites have been prepared from the reaction of alkylammonium-exchanged smectite clays with the diglycidyl ether of bisphenol-A and *m*-phenylenediamine (MPDA) as the curing agent by Pinnavaia and his coworkers [3]. They found that the monolithic exfoliated clay nanocomposite could be formed by pre-swelling alkylammonium ion exchanged forms of the clays with epoxy resin prior to curing, and a tremendous improvement in tensile strength and modulus was realized, particularly when the resin matrix exhibited a higher glass transition temperature. The curing kinetic of o-CFER/MeTHPA [4] and curing process of o-CFER/MeTHPA/O-MMT nanocomposite by isoconversional Methods [5] have been studied. But the descriptions of synthesis, isothermal curing kinetics and thermal degradation of o-CFER/MeTHPA/O-MMT nanocomposite have been lacking until now.

In general, kinetic expressions include two kinds of models: phenomenological and mechanistic. The phenomenological models are the *n*th-order reaction [6] and auto-catalytic model [7]. In this paper, Kamal's model [8] was applied to isothermal DSC data. In general, a good fit of experimental data was obtained in the early stages of the cure, but deviations were observed in the later stages, particularly near vitrification when the reaction was primarily diffusion controlled. To take into account the diffusion effect, the Kamal model was extended by the introduction of a diffusion factor, $f(\alpha)$. The structure changes during the curing process were investigated by infrared analysis (FTIR) and X-ray diffraction (XRD). The mechanism of thermal degradation was studied by means of thermogravimetric analysis (TGA) [9,10].

EXPERIMENTAL

Materials

Epichlorohydrin, o-cresol, formaldehyde, NaOH, KOH, acetone, ethyl alcohol, hydrochloric acid, 3-methyl-tetrahydrophthalic anhydride

(MeTHPA), N,N-dimethyl-benzylamine and $CH_3(CH_2)_{15}(CH_3)_3NBr$ were all analytically pure grade and were supplied by Beijing Chemical Reagent Co. Na^+-montmorillonite with the cation exchange capacity (CEC) value of about 100 mmol/100 g was purchased from Qingshan Chemistry Agent Factory in Lin'an (China).

Preparation of Organically Modified Montmorillonite

Twenty grams of Na^+-montmorillonite was dispersed into 500 mL of distilled water at 353 K. Nine grams of $CH_3(CH_2)_{15}(CH_3)_3NBr$ was dispersed in 100 ml distilled water, then was poured into the hot MMT/water solution and stirred vigorously for 1 h at 353 K. A white precipitate was formed, and separated by centrifugation, then washed several times with distilled water until no bromide was detected in the filtrate by one drop of 0.1 N $AgNO_3$ solution. The resulting O-MMT was dried in a convection oven at 353 K. The dried O-MMT was ground with a freezer/mill. The sieved O-MMT powder, less than 36 μm, was then to characterized.

Synthesis of o-cresol-formaldehyde Epoxy Resin (o-CFER)

Epoxy resin based on o-CFER was synthesized according to reference [11]. The linear o-cresol-formaldehyde resin synthesized in the first step was reacted with epichlorohydrin in the second step. The molecular structure of o-CFER has the following approximate form:

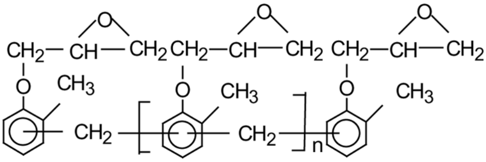

where $n = 1 \sim 3$. The epoxy value was determined according to Jay [12] to be 0.357 mol/100 g.

Synthesis of o-CFER/MeTHPA/O-MMT Nanocomposites

The o-CFER was mixed with the desired amount of O-MMT. The O-MMT was dispersed uniformly in o-CFER at 353 K for 2 h. Then, the curing agent was added to the hybrid and mixed thoroughly by stirring. The bubbles were removed from mixtures by vacuum after they were cast into a mold. The ratio of o-CFER and MeTHPA is 1:1 molar ratio of carboxyl group to epoxy group, and N,N-dimethylbenzylamine was used as a curing accelerant. The loadings of filler

O-MMT were 0, 3, and 7 phr (per 100 phr resins mixtures), respectively. The samples were cured for 2 h at 403 K and 4 h at 433 K.

IR Measurements

The o-CFER/MeTHPA/O-MMT samples were prepared with a stoichiometric ratio of one epoxy group to one carboxyl group. An FTS-40 IR spectrophotometer (FTIR, BIO-RAD Co., USA) was used to investigate the structural changes of the samples. The sample was dissolved in acetone, then coated as a thin film on a KBr plate. After the acetone was completely evaporated in vacuum, the sample was cured at 433 K. The non-cured sample, cured sample, the pristine montmorillonite and O-MMT were analyzed, separately.

X-ray Diffraction (XRD)

X-ray diffraction patterns were recorded by monitoring the diffraction angle 2θ from 1.5–10° on a RigakuD-max-γA-ray diffractometer. The diffractomter was equipped with a Cu*K*a ($\lambda = 0.1542\,\mathrm{nm}$) radiation source operated at 40 kV and 100 mA. The scanning speed and the step size used were 2°/min and 0.02°, respectively.

DSC Measurements

DSC analysis was carried out on a DT-41 differential scanning calorimeter (DSC) (Shimadzu Co. Ltd., Japan). The DSC instrument was calibrated with high-purity indium, α-Al_2O_3 was used as the reference material. Isothermal experiments were carried out according to Opalicki et al. [13] under a nitrogen flow of $40\,\mathrm{mL\ min^{-1}}$.

A 10 mg sample weighed accurately was placed in an aluminum DSC sample pan and sealed with an aluminum lid. The entire operation was carried out in a dry chamber. Isothermal DSC was performed at a series of curing temperatures T_c: 393 K, 398 K, 403 K and 408 K. The reaction was considered complete when the rate curve leveled off to the baseline. The total area under the exothermal curve, based on the extrapolated baseline at the end of reaction, was used to calculate the isothermal heat of cure, ΔH_i, at a given temperature. After each isothermal run, the sample was quenched rapidly to 283 K and then reheated at $10\,\mathrm{K\ min^{-1}}$ to 573 K in order to determine the residual heat of reaction, ΔH_r. The total heat evolved during the curing reaction is $\Delta H_0 = \Delta H_i + \Delta H_r$.

Thermogravimetric Analysis Measurement (TGA)

The sample was cured at 433 K for 4 h, and the thermal analysis was carried out on a Shimadzu DT-40 thermogravimetric analyzer under a static air atmosphere. About 3 mg of the sample, which had been completely cured, were put in a platinum cell and placed on the detector pan, then the furnace was heated to 923 K at a heating rate of 10 K min^{-1}.

RESULTS AND DISCUSSION

FTIR Analysis

The IR spectra (not shown here) of nanocomposites reveal the presence of characteristic absorptions of both inorganic and organic components. The absorption peaks at 1039 cm^{-1} and 796 cm^{-1} of MMT can be associated with Si-O-Si stretching vibrations. Absorption bands, on the other hand, at 3000–2800 cm^{-1} (CH_2 stretching), 1750 cm^{-1} (carbonyl group vibration), 1620–1436 cm^{-1} (aromatic C=C stretching), and 950–750 cm^{-1} (epoxy ring vibration) are consequences of the epoxy polymer. Especially, a new peak at 3000–2900 cm^{-1} appeared due to the CH_2 mode in the O-MMT. It is indicated that the MMT interlayer is organically modified by $CH_3(CH_2)_{15}(CH_3)_3NBr$. The most significant feature is the epoxide group absorption at 914 cm^{-1}. This absorption peak of o-CFER/MeTHPA/O-MMT cured for 600 min at 433 K becomes much lower than that of noncured o-CFER. In addition, the IR absorption in the carbonyl group of MeTHPA is a twinpeak about 1750 cm^{-1} before cure, but it became a single peak after cure. It shows that this reaction can be completed at 433 K for about 600 min.

X-ray Diffraction Analysis

The X-ray diffraction patterns for o-CFER/MeTHPA/O-MMT composites containing different content of O-MMT cured under the temperature of 433 K indicate that, as reported [14], when polymer chains are inserted into the galleries of montmorillonite, the lattice spacing is enlarged. These XRD patterns reveal the change in O-MMT basal spacing that occurs in the epoxy curing process. For the o-CFER/MeTHPA/O-MMT system, it is noteworthy that the (001) diffraction peak, corresponding to the basal spacing of montmorillonite d_{001}, shifted to a lower angle than that of O-MMT, and the peak intensity increased with increased loading of O-MMT. The X-ray diffraction peak occurs at $2\theta = 4.02^\circ$ for Org-MMT, and for the o-CFER/MeTHPA/O-MMT composite the diffraction peak shifted to $2\theta = 2.42^\circ \sim 2.46^\circ$. Obviously, an intercalated nanocomposite with the lattice spacing of $3.59 \sim 3.65\,\text{nm}$ (according to $2d\sin\theta = \text{n}\lambda$) was obtained. As Pinnavaia pointed out, the lattice spacing of the intercalated nanocomposite increases, but Bragg diffractions still exist in the diffractogram, which shifted to a lower angle. If the lattice spacing continues to increase, exfoliated nanocomposite is formed, will induce to the disappearance of Bragg diffraction.

The Heat (ΔH) of Cure Reaction of Nanocomposites

The DSC experiment was carried out by dynamic method, measuring the heat of different O-MMT contents according to the literature [9]. It was found that the addition of O-MMT had little effect on the reaction. In Table 1, it is indicated that the curing temperature region, enthalpy and curing time are all the same for o-CFER/MeTHPA and o-CFER/METHPA/O-MMT; obviously, an addition of O-MMT has no effect on the curing reaction of O-CFER/MeTHPA. However, due to the addition of O-MMT, the thermal stability, flame retardancy and mechanical properties were increased.

Isothermal Curing DSC

The mechanisms of the curing reaction of thermosetting resins have two general kinetic models: nth-order kinetics and autocatalytic kinetics [8]. The reaction rate of nth-order kinetics can be expressed as:

$$\frac{d\alpha}{dt} = K(T)(1-\alpha)^n \tag{1}$$

The reaction rate of autocatalytic kinetics can be defined as:

$$\frac{d\alpha}{dt} = k'\alpha^m(1-\alpha)^n \tag{2}$$

TABLE 1 Experimental Data of Cure Reaction

Sample	Temperature of peak/K			Enthalpy $\Delta H[J/g]$	Curing time t/min
	T_i	T_p	T_f		
o-CFER/MeTHPA	353	406	455	175.3	10
o-CFER/MeTHPA/O-MMT	353	407	456	174.5	10

Note: T_i, T_p, T_f are the initial, peak, and final temperature, respectively. The O-MMT content is 7%.

where α is the extent of reaction, given by $\alpha = \Delta H_t/\Delta H_0$, and ΔH_t is the partial area under a DSC trace up to time t; m and n are the reaction orders and k' is the kinetic rate constant.

To take into account the autocatalytic reaction, where the initial reaction rate of the autocatalytic reaction is not zero, Kamal [8] proposed the following generalized expression:

$$\frac{d\alpha}{dt} = (k_1 + k_2\alpha^m)(1-\alpha)^n \tag{3}$$

where k_1 and k_2 are the specific rate constants, which are functions of the temperature. According to the nth-order kinetic model, the maximum reaction rate will be observed at $t = 0$, and according to the autocatalytic model, the reaction rate is zero initially and attains the maximum value at some intermediate conversion.

During the curing reaction of epoxy resins, the heat evolution recorded by DSC is proportional to the extent of consumption of the epoxide groups, or the reactive groups in the curing agent, that is, the released heat is proportional to the extent of the reaction. Following this assumption, the curing kinetics were studied, and the kinetics data were determined. If the cure reaction is the only thermal event, then the reaction rate $d\alpha/dt$ is proportional to the heat flow, dH/dt, that is:

$$\frac{d\alpha}{dt} = \frac{dH/dt}{\Delta H_0} \tag{4}$$

The rate of the curing reaction can be determined by the curing exotherm. Figure 1 shows plots of the curing reaction conversion α versus time t at different isothermal temperatures, and the plots of $d\alpha/dt$ versus time t are shown in Figure 2. As seen from Figures 1 and 2, the reaction rate at any temperature increases with time at the initial stage of cure and passes through a maximum. The peak of reaction rate becomes higher and shifts to shorter time with an increasing curing temperature, but the conversion α reaches only about $80 \sim 90\%$ in the experiment time. The plots show a maximum reaction rate at time $t > 0$, thereby negating simple nth-order kinetics. To compute kinetic parameters in Eq. 4, several methods have been proposed [15,16]. In this study, k_1 was graphically calculated as the initial reaction rate at time $t = 0$, given by the intercept of Figure 2. Then, k_2, m and n were calculated through non-linear regression according to Eq. 3. The resulting data are shown in Table 2.

It can be seen from Table 2 that k_1 values are small compared with those obtained for k_2, which affects the reaction more. Furthermore, k_1 and k_2 values increase with rising curing temperatures. The reaction

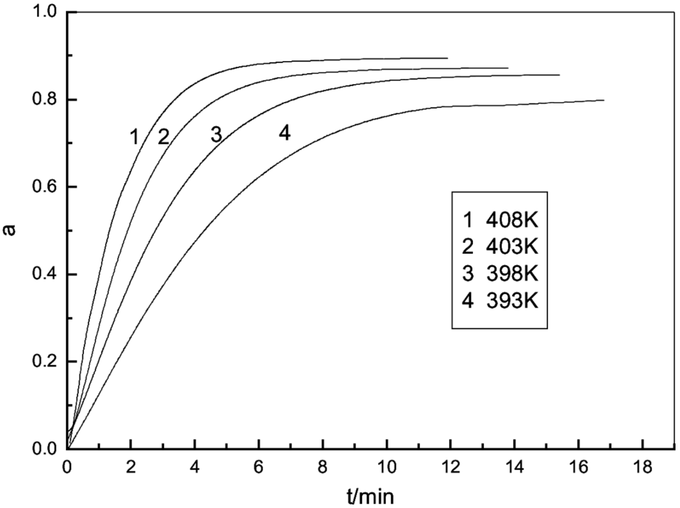

FIGURE 1 Conversion, α versus time plots at different curing temperatures.

rate constants k_1 and k_2 depend on the temperature and follow the Arrhenius relationship:

$$k_i = A_i \exp(-E_i/RT) \quad i = 1, 2 \tag{5}$$

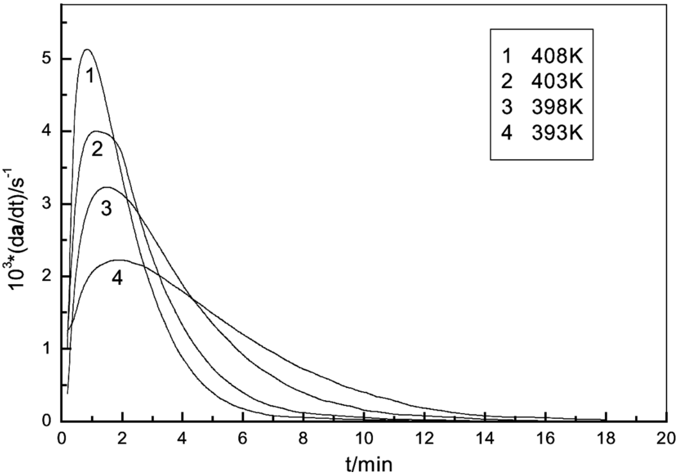

FIGURE 2 Reaction rate, $d\alpha/dt$ versus time plots at different temperatures.

TABLE 2 Kinetic Parameters for Isothermal Curing Reaction of o-CFER/MeTHPA/O-MMT

T (K)	393	398	403	408
k_1 ($\times 10^{-4}/\mathrm{S}^{-1}$)	2.03	6.02	11.73	20.94
k_2 ($\times 10^{-3}/\mathrm{S}^{-1}$)	4.68	7.21	12.02	18.83
m	0.38	0.45	0.47	0.76
n	1.17	1.26	1.44	1.89

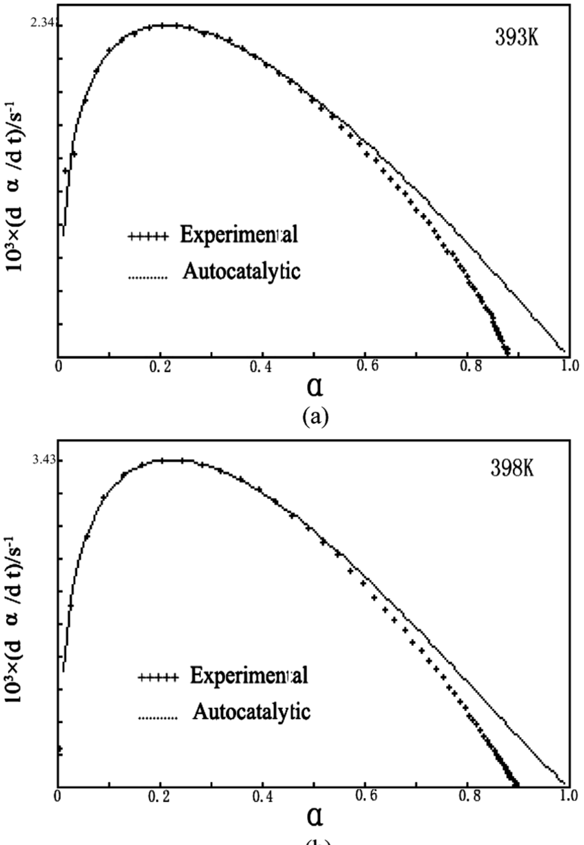

(a)

(b)

FIGURE 3 Comparison of experimental data with theoretical values: plots of reaction rate $d\alpha/dt$ versus conversion α at 393 K and 398 K.

where A_i is the pre-exponential constant, E_i is the activation energy, R is the gas constant, and T is the absolute temperature. When the constants k_1 and k_2 are used in an Arrhenius plot, the values of the associated activation energies, E_1 and E_2, are 188.94 kJ/mol and 114.93 kJ/mol, respectively. The linear correlation coefficient is 0.9973 for k_1 values and 0.9958 for k_2.

Typical comparisons between the experimental DSC data for the two different temperatures 393 K and 398 K, and the autocatalytic model with Eq. 3 determined parameters, are shown in Figure 3. The kinetics behavior described by the kinetic model coincides with the experimental data in the early stage. As the reaction progresses, a deviation appears due to the onset of gelation and vitrification where the mobility of reactive groups is hindered, and the rate of conversion is controlled by diffusion rather than by kinetic factors [17]. Differences between model predictions and experimental data were observed. This can be interpreted in terms of free volume considerations [18]. The free volume of the materials decreases with temperature and the rate of diffusion of reactive groups is reduced, leading to decreasing reaction rate.

To consider the diffusion effect more precisely, a semiempirical relationship, based on free volume considerations, was proposed by Chern [18]. In this relationship, a diffusion factor, $f(\alpha)$, is defined with

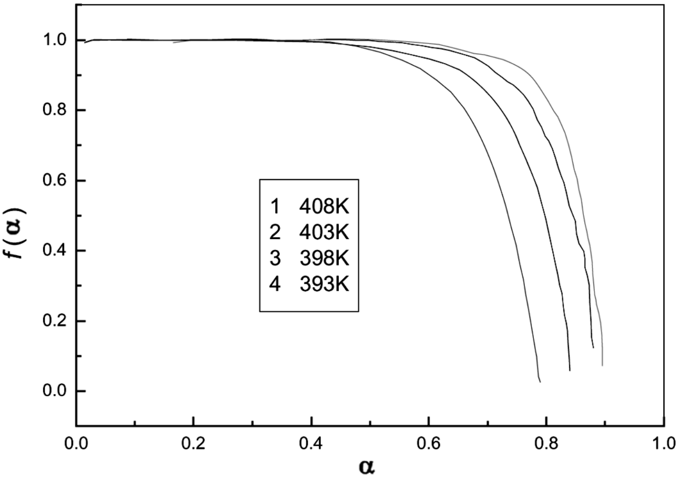

FIGURE 4 Plots of diffusion factor $f(\alpha)$ versus conversion α at different curing temperature.

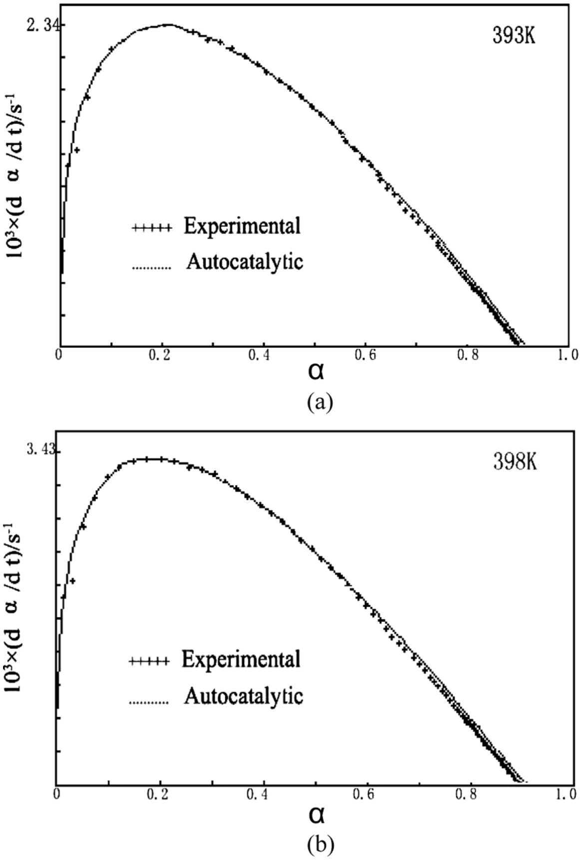

(a)

(b)

FIGURE 5 Comparison of experimental data with theoretical values calculated from Eq. 7: reaction rate $d\alpha/dt$ versus conversion α at 393 K and 398 K.

two empirical parameters as follows:

$$f(\alpha) = \frac{1}{1 + \exp[C(\alpha - \alpha_c)]} \tag{6}$$

where C is the diffusion coefficient and α_c is the critical conversion depending on the curing temperature. The plots of $f(\alpha)$ versus conversion α at different curing temperatures are shown in Figure 4. For $\alpha \ll \alpha_c$, $f(\alpha)$ approximately equals unity and the effect of diffusion is negligible, so that the reaction is kinetically controlled. As α approaches α_c, $f(\alpha)$ begins to decrease, reaching a value of 0.5 at $\alpha = \alpha_c$. Beyond that point, it continues to decrease and approaches

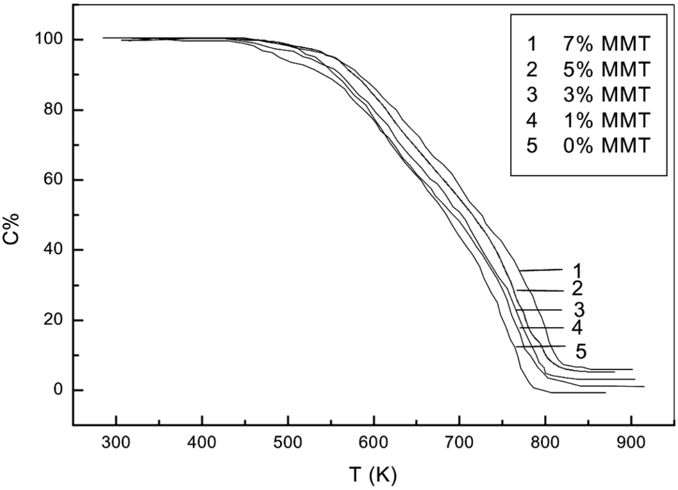

FIGURE 6 The thermal degradation curves of nanocomposites with different O-MMT content.

zero, which means that the reaction becomes very slow and effectively stops.

Considering the diffusion effect, the kinetic equation of cure can be expressed in the following form to account for the effects of diffusion.

$$\frac{d\alpha}{dt} = (k_1 + k_2\alpha^m)(1-\alpha)^n \cdot \frac{1}{1+\exp[C(\alpha-\alpha_c)]} \tag{7}$$

Figure 5 shows a comparison between experimental values and those obtained from Eq. 7. The calculated values agree very well with experimental data under higher temperature [4]. Therefore, we employ the proposed generalized kinetic model to predict and describe the advance of this epoxy resin systems as a function of the curing temperature.

Thermal Degradation

The process of the weight loss is shown in Figure 6. It can be seen that with increased of O-MMT content, TG curves shift to high temperature, and the corresponding temperatures $T_{\max}$ at the maximal degradation velocity increase, too. When the content of O-MMT is 7%, the $T_{\max}$ are higher by 33.6 K than that of pure o-CFER/MeTHPA system. The thermal stability of composites improved, because the layers of O-MMT suppress effectively the emanation of small molecules when degradation reaction originates, resulting in the decrease of degradation velocity of the composites. In addition, the stronger interaction between o-CFER and O-MMT suppresses the mobility of the macromolecule chains, slowing the diffusion of volatiles and the degradation process.

CONCLUSIONS

The XRD indicates that the epoxy resin molecules had inserted into the galleries of montmorillonite, and an exfoliated nanocomposite was obtained. The O-MMT did not change the reaction mechanism of o-CFER/MeTHPA. Similar to o-CFER/MeTHPA, the curing reaction of o-CFER/MeTHPA/O-MMT system shows an autocatalytic kinetic behavior in the kinetically controlled stage and can be well-described with the model proposed by Kamal. The curing reaction at the later stage was practically diffusion-controlled. The diffusion factor $f(\alpha)$ could be introduced into Kamal's equation to make it possible to describe and predict the curing reaction of epoxy resins. When increasing O-MMT content, the TG curves shift to high temperature, and corresponding temperatures at the initial degradation and at the maximal degradation velocity increased, too.

REFERENCES

[1] Lan, T., Kaviratna, P. D., and Pinnavaia, T. J., *Chem. Mater.* **7**, 2144 (1995).

[2] Kornmann, X., Lindberg, H., and Berglund, L. A., *Polym.* **42**, 4493 (2001).

[3] Lan, T., Kaviratna, P. D., and Pinnavaia, T. J., *Proc. ACS, Div. Polym. Mater. Sci. Eng.* **71**, 528 (1994).

[4] Gao, J. G., Zhao, M., and Li, Y. F., *Inter. J. Polym. Mater.* **55**, 1009 (2006).

[5] Gao, J. G., Zhao, M., and Qin, J. L., *Ir. Polym. J.* **15**, 425 (2006).

[6] Deng, B. L., Hu, Y. S., Chen. L. W., Chiu, W. Y., and Wu, T. R., *J. Appl. Polym. Sci.* **74**, 229 (1999).

[7] Lam, P. W. K., Plaumann, H. P., and Tran, T., *J. Appl. Polym. Sci.* **41**, 3043 (1990).

[8] Kamal, M. R., *Polym. Eng. Sci.* **14**, 23 (1974).

[9] Liu, Z. H. (1991). *Introduction of Thermal Analysis*, Beijing, Chem. Ind. Publish. Co.

[10] Madhusudanan, P. M., Krishnan, K., and Ninan, K. N., *Thermochim Acta* **97**, 189 (1986).

[11] Ren, L. B., *Chinese Thermosetting Resin* **13**, 17 (1998).

[12] Jay, R. R., *Anal. Chem.* **36**, 665 (1964).

[13] Opalicki, M., Kenny, J. M., and Nicolais, L., *J. Appl. Sci.* **61**, 1025 (1996).

[14] Kornmann, X., Lindberg, H., and Berglund, L. A., *Polym.* **42**, 1303 (2001).

[15] Ryan, M. E. and Dutta, A., *Polym.* **20**, 203 (1979).

[16] Kenny, J. M., *J. Appl. Polym. Sci.* **51**, 761 (1994).

[17] Cole, K. C., Hechler, J. J., and Noel, D., *Macromolecules* **24**, 3098 (1991).

[18] Chern, C. S. and Poehlein, G. W., *Polym. Eng. Sci.* **27**, 782 (1987).